Automatic slice thickness measurement on computed tomography images of American College of Radiology phantom

Choirul Anam[1], Dewi A. Insiano[1], Eko Hidayanto[1], Ariij Naufal[1], Annisa Tenri Maya[2], Tunggul Drajat Mulatomo[2], Mohd Hanafi Ali[3]

[1]Department of Physics, Faculty of Science and Mathematics, Diponegoro University, Semarang, Indonesia
[2]Loka Pengamanan Fasilitas Kesehatan (LPFK), Surakarta, Indonesia
[3]Faculty of Medicine, Lincoln University College, Selangor, Malaysia

Article Info

ABSTRACT

This study aims to develop an automatic method for calculating slice thickness on an American College of Radiology (ACR) phantom and evaluate its accuracy at variations of orientation angle and slice thickness. The phantom was scanned using Siemens SOMATOM perspective, with variations of the slice thickness (i.e. 1.5, 3, 5, 6, 7, and 10 mm) and rotation angles (i.e. 0.0, 22.5, 45.0, and 67.5°). The phantom rotation was based on the bone object as a reference. After determining the rotation angle, the phantom image was rotated by the angle. Next, profiles of pixel values across the wire objects for measuring slice thickness were developed from rotated phantom images. The slice thickness was measured automatically from the obtained profiles. The results of the automated method are 2.5, 4.1, 5.4, 5.8, 7.8, and 9.8 mm for all varied slice thicknesses. The differences between the automatic and manual methods are within 0.3 mm. The automatic method is capable of detecting slice thickness for various angles. The differences in slice thickness for various angles are within 0.1 mm for a slice thickness of 3 mm. These results are similar when compared to manual measurements. An algorithm for automated slice thickness measurement on ACR phantom has been successfully developed.

Corresponding Author:

Choirul Anam
Department of Physics, Faculty of Science and Mathematics, Diponegoro University
Prof. Soedarto SH Street, Tembalang, Semarang 50275, Central Java, Indonesia
Email: anam@fisika.fsm.undip.ac.id

1. INTRODUCTION

Computer tomography (CT) is widely used in health services worldwide. CT is a non-destructive imaging modality that can provide detailed information about the internal structure of patients using a combination of X-ray radiation and a sophisticated computer system [1], [2]. By utilizing CT, images of the brain, neck, chest, spine, pelvis, abdomen, skull base, sinuses, auditory canal, cervical spine, thoracic spine, lumbar spine, and many other patient's bodies can be easily obtained [3], [4]. CT displays anatomical images of the body clearly in axial, coronal, and sagittal planes [5], [6].

CT image quality is quantified by many parameters including spatial resolution [7]–[9], contrast resolution [10], and noise [11]. Good image quality can provide relevant information to help medical personnel to provide accurate diagnostic results to patients [12]. Because slice thickness has a direct impact on noise level [13] and image spatial resolution [14], it is one main parameter that determines image quality [13]. Thin slices are usually used for the examination of small organs or anomalies because they provide a

more detailed image [15], [16]. The slice thickness of CT images typically ranges from sub-millimeters to 5 mm, depending on the anatomy being scanned [17].

Slice thickness can be measured on specifically designed phantoms such as the American College of Radiology (ACR) CT [18], [19] or American Association of Physicists in Medicine (AAPM) CT performance [20] or Catphan phantoms [21], [22]. Medical staff usually measure slice thickness manually based on their expertise and experiences. It is worth noting that manual measurements have some drawbacks, i.e. dependent on the subjectivity of the human observer. Therefore, efforts to develop an objective measurement method were carried out.

Lasiyah *et al.* [23] proposed an automatic measurement of slice thickness on the AAPM CT performance phantom (CIRS, Virginia, USA). The results showed that the developed algorithm is valid and capable of producing very accurate measurement results. Karius and Bert [24] proposed an automatic slice thickness on the Catphan phantom. Automatic CT Software (ACTS) (Gammex Inc.) was used to automatically measure the slice thickness of the ACR CT phantom. However, the ACTS is not widely owned by health services because the price is expensive. In addition, the available software had limitations. One of them is that it can only estimate slice thickness for the exact position [25]. If the image to be analyzed has a slight angle rotation, the automation cannot measure the slice thickness.

It is worth noting that there is a holder for helping to accurately locate the ACR CT phantom. However, in practice, it is still difficult to exactly and accurately locate the phantom in the proper position. Medical personnel sometimes need to scan the phantom many times to obtain the proper position so that the software can automatically measure the slice thickness. Based on these issues, we developed an automated tool for measuring slice thickness on ACR CT phantom images that can adjust to the phantom orientation angle. Our method will help to allow ACR CT phantom positioning with misalignment tolerance, thus facilitating fast and flexible image acquisition. To prove the robustness of the method, the proposed method was tested on various nominal slice thicknesses and phantom orientation angles.

2. RESEARCH METHOD

2.1. Phantom image

ACR CT phantom was scanned with a Siemens Somatom perspective CT scanner. The phantom was scanned with various slice thicknesses from 1.5 mm up to 10 mm for angle 0°, and for slice thickness of 3 mm, the phantom was scanned with four different angles. The scan parameters are shown in Table 1.

Table 1. Scan parameters

Parameters	Slice thickness variation	Rotation angle variation
Acquisition mode	Helical	Helical
Tube voltage (kV)	110	110
Tube current (mA)	100	100
Pitch	1.0	1.0
Field of view (FOV) (mm)	204	204
Reconstruction filter	Medsternum	Medsternum
Rotation time (s)	1.0	1.0
Slice thickness (mm)	1.5, 3, 5, 6, 7, 10	3
Phantom rotation angle (^{0})	0	0, 22.5, 45, 67.5

2.2. Automatic slice thickness measurement

Figure 1 illustrates all steps of the automatic measurement of slice thickness on the ACR CT phantom. Automated measurement of slice thickness on ACR CT phantoms follows a similar principle to the manual method, which involves counting the wire objects visible on the axial image of the phantom. The thicker slice thickness leads to more identified wire objects by the observer. However, the number of identified objects depends on the observer's interpretation. The goal of the automated method is to identify the number of wire objects using a universal threshold to minimize subjectivity.

Initially, the image was opened using a graphical user interface (GUI) built on Python programming language (Figure 1(a)). Then, we determined the orientation angle of the phantom using a bone object as a reference (Figure 1(b)). To achieve the orientation angle of the phantom, the center of the phantom and the center of the bone object were determined. The bone's centroid was then determined after the bone was segmented using a threshold value of 800 HU to produce a binary image, i.e. the bone object had a value of 1 and the background had with value of 0. After determining the centroids of phantom and bone, the angle between the lines of the two centroids and the vertical line was determined. After determining the angle of rotation, the image of the phantom was rotated by the angle (Figure 1(c)). This procedure generated an image

with a zero-degree rotation angle. Next, the profiles of pixel values across the wire objects for measuring slice thickness were developed from the rotated phantom image (Figure 1(d)). In this case, we developed two profiles at the right and left wire objects, and the result was calculated as the average of the two profiles. To automatically measure slice thickness, we normalized the profiles first (Figure 1(d)). It was noted that the profiles were different from small and wide slice thickness due to partial volume artifacts (PVA), i.e., the top of the profile of small slice thickness had a higher value than the wide slice thickness. After that, we omitted noise from the profiles using a threshold value of 0.2, such that any values of profiles greater than 0.2 will be converted to 1 (Figure 1(e)), and those below 0.2 will be converted to 0. Finally, the peaks of profiles were automatically counted (n) by labeling them and it directly indicated the slice thickness (Figure 1(f)). The final slice thickness was calculated as the average of the slice thickness from left and right wire objects.

The determination of rotation angle is illustrated in Figure 2. In the case where the phantom was not rotated (rotation angle = 0°), the two lines produced 45° (Figure 2(a)). Therefore, the rotation angle was determined by subtracting 45° from these two lines (Figure 2(b)). This automatic method can be accessed by clicking the "calculate" button. Similar to previous studies [13], [23], for many images coming from different datasets, this method can be replicated easily as the input parameters can be customized according to the user's needs. The results obtained are also clearly displayed in the results column. To verify the automatic measurement results, the user can count the objects visible in the image displayed on the screen directly.

(a)

(b)

(c)

(d)

(e)

(f)
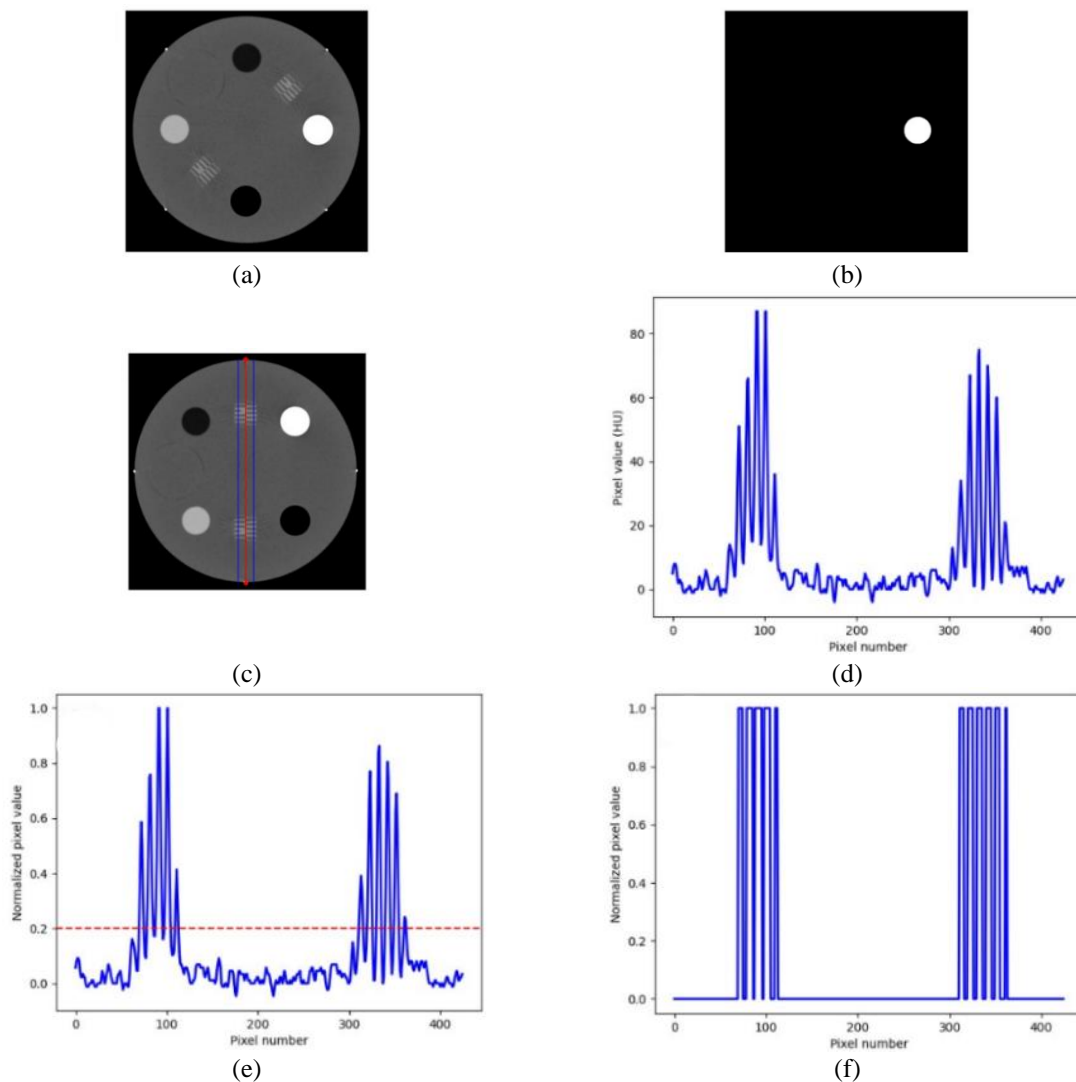
Figure 1. Stages of automatic slice thickness measurement, (a) original image, (b) image of the segmented bone object as reference for angle determination, (c) lines for developing pixel profile of pixel values for determining slice thickness on the rotated phantom, (d) resulted in profile of pixel values, (e) red line for thresholding resulted in profile for deleting noise, and (f) profile after deleting noise. the peaks of the profile were counted to determine the slice thickness of the image

(a)   (b)
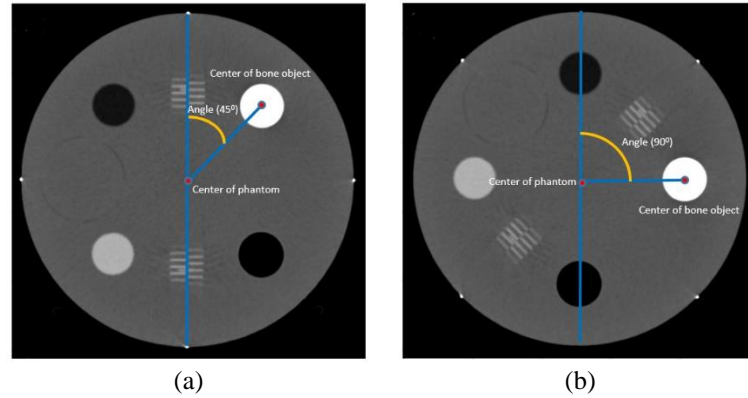
Figure 2. Angle determination using the center of the bone object as reference for ACR CT phantom, an
example of the phantom with the angle of (a) 0.0° and (b) 45°

In the current study, the automated slice measurement was to be implemented for measuring slice thickness with various nominal slice thicknesses and angle rotations. Measurements were performed at five locations. The average and standard deviation (SD) were calculated.

3.   RESULTS AND DISCUSSION
3.1. Variations in slice thickness

Figure 3 shows the images with lines along the object of wires to obtain profiles for various slice thicknesses of 1.5 mm (Figure 3(a)), 3 mm (Figure 3(b)), 5 mm (Figure 3(c)), 6 mm (Figure 3(d)), 7 mm (Figure 3(e)), and 10 mm (Figure 3(f)). It appears that the lines along the object of wires to obtain profiles are in the right position for all variations of slice thickness. The results of the measured slice thickness are tabulated in Table 2. Figure 4 depicts the relationship between nominal and measured slice thicknesses. We found that the measured slice thickness correlates linearly with the nominal slice thickness for automatic method $R^2=0.9778$ and manual method $R^2=0.9785$. This means that the automatic and manual methods produce similar results for various nominal slice thicknesses.

(a)   (b)   (c)

(d)   (e)   (f)
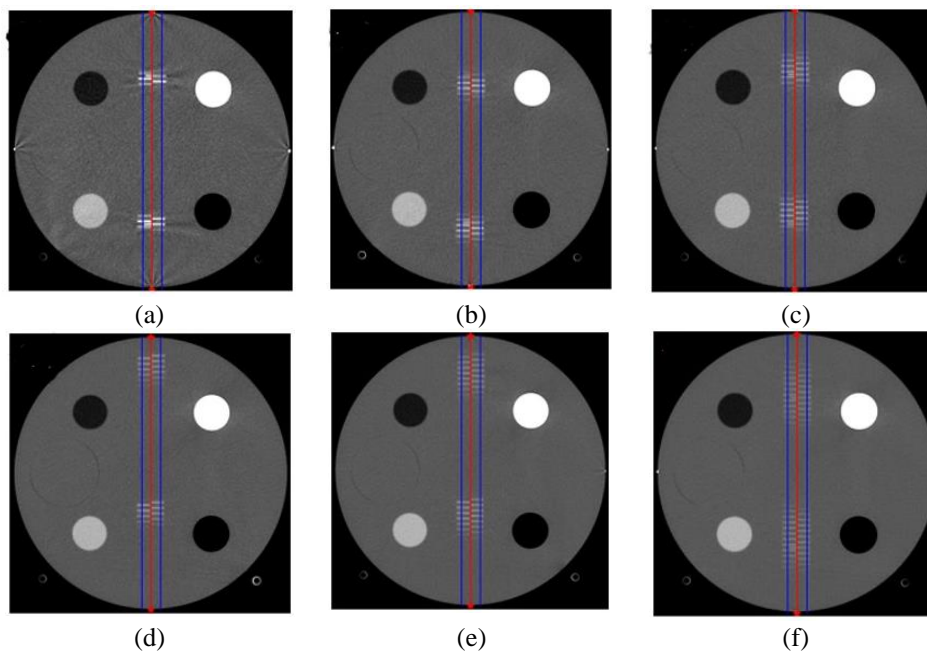
Figure 3. Images with two lines to obtain profiles along the object of wires for various slice thicknesses:
(a) 1.5 mm, (b) 3 mm, (c) 5 mm, (d) 6 mm, (e) 7 mm, and (f) 10 mm

Table 2. Results of automated slice thickness measurement for various slice thickness

Nominal slice thickness	Automatic method (mm)	Manual method (mm)	Difference (mm)
1.5	2.5±0.3	2.2±0.1	0.3
3	4.1±0.6	4.0±0.5	0.1
5	5.4±0.5	5.1±0.6	0.3
6	5.8±1.2	5.7±1.0	0.1
7	7.8±0.6	7.6±0.6	0.2
10	9.8±1.1	9.7±0.0	0.1
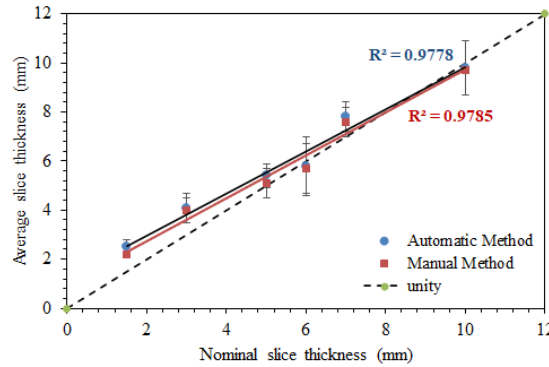
Figure 4. Correlation between nominal and measured slice thicknesses (automatic method and manual method)

3.2. Variation in angle rotation

Figure 5 (first row) shows the images of the phantom scanned for fix nominal slice thickness of 3 mm and with rotation angles of 0° (Figure 5(a)), 22.5° (Figure 5(b)), 45° (Figure 5(c)), and 67.5° (Figure 5(d)). The second row of Figure 5 shows the rotated images of the phantom with different angle rotations. The images of the phantom are accurately rotated. We were able to position a phantom with a very high orientation angle error, although this rarely happens in real scenarios. It also indicates the lines (blue lines) to obtain the profile of the wire object for measuring slice thickness. The results of slice thickness for various angle rotations are tabulated in Table 3. We found that in various angles, the automatic method produced similar results as the manual method, with a maximum difference is 0.3 mm.

(a)	(b)	(c)	(d)
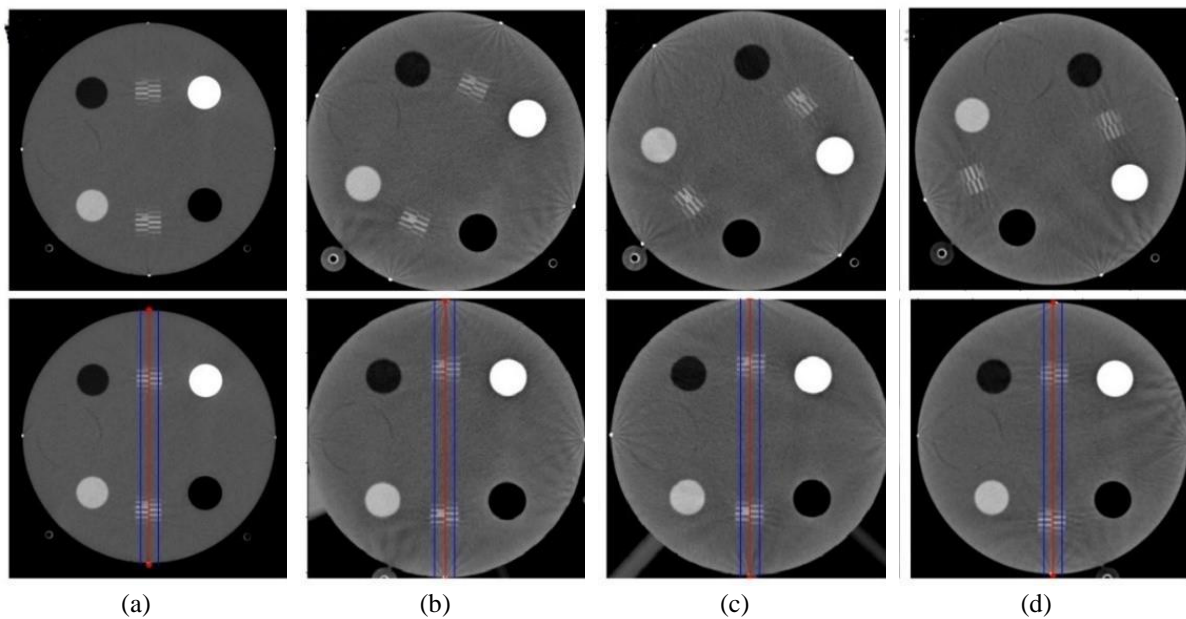
Figure 5. Original mages (first row) and rotated images with lines for developing profiles along the object of wires for different angle variations: (a) 0.0°, (b) 22.5°, (c) 45°, and (d) 67.5°

Table 3. Results of automated slice thickness measurement for fixed nominal slice thickness of 3 mm and for various angle rotation slice thickness

Nominal slice thickness (mm)	Angle (degree)	Automatic method (mm)	Manual method (mm)	Difference (mm)
3	0.0	4.0±0.7	4.0±0.1	0.0
3	22.5	4.2±0.6	3.9±0.1	0.3
3	45.0	4.0±0.2	3.9±0.1	0.1
3	67.5	4.1±0.3	4.0±0.1	0.1

This research aims to develop an automatic software for measuring the slice thickness in ACR CT phantom at different slice thicknesses and orientation angles. For clinical purposes, what is needed is not software that can measure slice thickness with large angle variations, because the ACR CT phantom has a system to help position the phantom properly. If there is an inaccuracy in the phantom position, for example, it has a certain angle, it is usually a very small angle. However, existing software usually fails to detect slice thickness with that small angle [25]. The current proposed software can detect angles, whether large or small angles. With this software, it will be easier for medical personnel to perform slice thickness measurements automatically. Medical personnel are still recommended to place the phantom as accurately as possible. However, if there is a slight inaccuracy in the phantom position, i.e. there is a small angle, medical personnel do not have to repeat the measurement because the software can still measure slice thickness accurately.

In this study, slice thickness measurement is performed automatically from the wire's object profile. First, the object is normalized to make it easier to determine the threshold value. If it is not normalized, the peak value of the profile will be greatly influenced by the slice thickness value due to the PVA phenomenon. For small slice thickness, the profile peak value will be much higher, compared to the profile peak at large slice thickness. By performing the normalization process, regardless of the slice thickness value, the peak value is equal to one. After that, the profile is segmented with a threshold value of 0.2. This means that for a profile value of more than 0.2, it will be converted to a value of 1, and for a profile value of less than 0.2 it will be converted to a value of 0. For the initial study, this threshold value has given quite good results. However, further studies are needed to determine the most optimal threshold value. Next, the slice thickness value is measured based on the number of objects with a value of 1 using the labeling process.

The results obtained in this study are shown in Figure 4. The nominal slice thickness values used are 1.5, 3, 5, 6, 7, and 10 mm. The results for the automatic method are 2.5, 4.1, 5.4, 5.8, 7.8, and 9.8 mm, while for the manual method are 2.2, 4.0, 5.1, 5.7, 7.6, and 9.7 mm. The correlation coefficient values obtained from each method are $R^2=0.9778$ and $R^2=0.9785$. Based on these results, the linearity obtained is quite good because it is close to 1. Based on Table 2, the difference between nominal and measured slice thickness is about 1 mm or less.

Another approach that can be taken to automatically measure slice thickness is to detect several peaks in the profile, and the full width at half maximum (FWHM) of the profile is measured. This approach might get more accurate results and this approach can be done without having to use a threshold value that may not be appropriate for certain cases. Several studies have used FWHM measurements on aluminum ramps to measure slice thickness [23], [24]. Although the structure of the aluminum ramp and wire ramp are different, the FWHM measurement can be applied to both. Slice thickness measurement on the ACR phantom by measuring the value of the FWHM profile, will be carried out in the next study.

Table 3 shows the results of automatic measurements for four variations of rotation, namely 0.0°, 22.5°, 45.0°, and 67.5° for a nominal slice thickness of 3 mm. The measured slice thicknesses are 4.0, 4.2, 4.0, and 4.1 mm, respectively. In comparison, the results of the manual measurement are 4.0, 3.9, 3.9, and 4.0 mm, respectively. It can be seen that the difference between manual and automated methods is less than 0.3 mm. This shows that the automatic calculation of the slice thickness with the proposed method is accurate even if the object angle is not in zero position.

In the proposed method, the phantom angle is detected using the reference position of the bone object. This bone object was chosen because of the easiness of segmenting the object because the bone has a CT number of +850 HU to +970 while the background is water with a CT number of around 0 HU. In addition to the bone object, the air object in the phantom is also very easy to segment and can be used as a references, because the air object has a CT number of around -1,000 HU. On the other hand, polyethylene and acrylic objects are relatively more difficult to segment because they have a different CT number with a background of only about 100 HU. In the beginning, we considered using a small radio-opaque object (for locating phantom at the center gantry) that is at the edge of the phantom, but sometimes the object is not visible due to several things such as: first, the image is cropped due to the FOV being too small or due to improper centering, and secondly the phantom position is slightly tilted, which causes the BB object to not exist in the image, especially at small slice thicknesses. For this reason, we did not use the BB object and instead used the bone object which is located inside the phantom as a reference. By using bone object as a

reference, this software can accurately detect the position of the slice thickness object for several variations used in this study. However, comprehensive testing for other variations needs to be performed in future studies.

The limitation of this study lies in the image rotation process. Although this process does not cause artifacts that affect the measurement results, there is a concern that it alters the pixel profile of the wire object. It would be better if the automated method could adjust the orientation angle of the phantom without counter-rotating the image. This will be implemented in our next study.

4. CONCLUSION

A method for automated slice thickness measurement with various ACR CT phantom angles has been successfully developed. The results of the automated method are 2.5, 4.1, 5.4, 5.8, 7.8, and 9.8 mm for nominal slice thicknesses of 1.5, 3, 5, 6, 7, and 10 mm, respectively. The differences between the automatic and manual methods are within 0.3 mm. The results of the automated method of nominal slice thickness of 3 mm for various angles of 0.0°, 22.5°, 45.0°, and 67.5° are 4.0, 4.2, 4.0, and 4.1 mm, respectively. Compared to the manual method, our automatic method produced similar results in various nominal slice thicknesses and phantom orientations. Due to its easy nature on ACR CT phantom images with flexible misalignment tolerances, our method can help medical personnel perform QA procedures in healthcare facilities efficiently.

REFERENCES

[1]   N. I. Khoirina, Y. Kartikasari, and S. Sudiyono, "Differences in anatomical image quality on computed tomography angiography (CTA) abdominal aorta with variation of threshold values (in Indonesian)," *Jurnal Riset Kesehatan*, vol. 5, no. 2, pp. 65–72, Sep. 2017, doi: 10.31983/jrk.v5i2.1237.
[2]   P. J. Withers *et al.*, "X-Ray computed tomography," *Nature Reviews Methods Primers*, vol. 1, no. 1, Feb. 2021, doi: 10.1038/s43586-021-00015-4.
[3]   M. Moradi, Y. Gur, H. Wang, P. Prasanna, and T. Syeda-Mahmood, "A hybrid learning approach for semantic labeling of cardiac CT slices and recognition of body position," in *2016 IEEE 13th International Symposium on Biomedical Imaging (ISBI)*, IEEE, Apr. 2016, pp. 1418–1421. doi: 10.1109/ISBI.2016.7493533.
[4]   C. P. Dimitroukas, V. I. Metaxas, F. O. Efthymiou, C. P. Kalogeropoulou, P. E. Zampakis, and G. S. Panayiotakis, "Patient dose audit in common CT examinations," *Radiation Physics and Chemistry*, vol. 192, Mar. 2022, doi: 10.1016/j.radphyschem.2021.109924.
[5]   C. M. Davis *et al.*, "Is there asymmetry between the concave and convex pedicles in adolescent idiopathic scoliosis? a CT investigation," *Clinical Orthopaedics & Related Research*, vol. 475, no. 3, pp. 884–893, Mar. 2017, doi: 10.1007/s11999-016-5188-2.
[6]   J.-P. Grunz *et al.*, "The importance of radial multiplanar reconstructions for assessment of triangular fibrocartilage complex injury in CT arthrography of the wrist," *BMC Musculoskeletal Disorders*, vol. 21, no. 1, Dec. 2020, doi: 10.1186/s12891-020-03321-2.
[7]   J. Wang and D. Fleischmann, "Improving spatial resolution at CT: development, benefits, and pitfalls," *Radiology*, vol. 289, no. 1, pp. 261–262, Oct. 2018, doi: 10.1148/radiol.2018181156.
[8]   T. Higaki, Y. Nakamura, F. Tatsugami, T. Nakaura, and K. Awai, "Improvement of image quality at CT and MRI using deep learning," *Japanese Journal of Radiology*, vol. 37, no. 1, pp. 73–80, Jan. 2019, doi: 10.1007/s11604-018-0796-2.
[9]   J. J. Foy *et al.*, "Harmonization of radiomic feature variability resulting from differences in CT image acquisition and reconstruction: assessment in a cadaveric liver," *Physics in Medicine and Biology*, vol. 65, no. 20, Oct. 2020, doi: 10.1088/1361-6560/abb172.
[10]   J. C. Infante, Y. Liu, and C. K. Rigsby, "CT image quality in sinogram affirmed iterative reconstruction phantom study – is there a point of diminishing returns?," *Pediatric Radiology*, vol. 47, no. 3, pp. 333–341, Mar. 2017, doi: 10.1007/s00247-016-3745-1.
[11]   L. Lechuga and G. A. Weidlich, "Cone beam CT vs. FAN beam CT: a comparison of image quality and dose delivered between two differing CT imaging modalities," *Cureus*, vol. 8, no. 9, Sep. 2016, doi: 10.7759/cureus.778.
[12]   H. Elnour, H. Ahmed Hassan, A. Mustafa, H. Osman, S. Alamri, and A. Yasen, "Assessment of image quality parameters for computed tomography in Sudan," *Open Journal of Radiology*, vol. 07, no. 01, pp. 75–84, 2017, doi: 10.4236/ojrad.2017.71009.
[13]   C. Anam *et al.*, "Automatic slice thickness measurement on three types of catphan CT phantoms," *Biomedical Physics and Engineering Express*, vol. 9, no. 4, Jul. 2023, doi: 10.1088/2057-1976/acd785.
[14]   G. Vermiglio, G. Acri, B. Testagrossa, F. Causa, and M. Giulia, "Procedures for evaluation of slice thickness in medical imaging systems," in *Modern Approaches to Quality Control*, London, United Kingdom: InTech, 2011. doi: 10.5772/23693.
[15]   F. Morsbach, Y.-H. Zhang, L. Martin, C. Lindqvist, and T. Brismar, "Body composition evaluation with computed tomography: contrast media and slice thickness cause methodological errors," *Nutrition*, vol. 59, pp. 50–55, Mar. 2019, doi: 10.1016/j.nut.2018.08.001.
[16]   J. T. Bushberg, J. A. Seibert, E. M. Leidholdt, and J. M. Boone, *The essential physics of medical imaging*, Third Edit., vol. 40, no. 7. PA, USA: Lippincott Williams and Wilkins, Philadelphia, 2013. doi: 10.1118/1.4811156.
[17]   J. M. Ford and S. J. Decker, "Computed tomography slice thickness and its effects on three-dimensional reconstruction of anatomical structures," *Journal of Forensic Radiology and Imaging*, vol. 4, pp. 43–46, Mar. 2016, doi: 10.1016/j.jofri.2015.10.004.

[18] T. M. Ihalainen *et al.*, "MRI quality assurance using the ACR phantom in a multi-unit imaging center," *Acta Oncologica*, vol. 50, no. 6, pp. 966–972, Aug. 2011, doi: 10.3109/0284186X.2011.582515.

[19] Z. Mansour, A. Mokhtar, A. Sarhan, M. T. Ahmed, and T. El-Diasty, "Quality control of CT image using american college of radiology (ACR) phantom," *The Egyptian Journal of Radiology and Nuclear Medicine*, vol. 47, no. 4, pp. 1665–1671, Dec. 2016, doi: 10.1016/j.ejrnm.2016.08.016.

[20] J. Bissonnette *et al.*, "Quality assurance for image-guided radiation therapy utilizing ct-based technologies: a report of the AAPM TG-179," *Medical Physics*, vol. 39, no. 4, pp. 1946–1963, Apr. 2012, doi: 10.1118/1.3690466.

[21] M. Alshipli and N. A. Kabir, "Effect of slice thickness on image noise and diagnostic content of single-source-dual energy computed tomography," *Journal of Physics: Conference Series*, vol. 851, May 2017, doi: 10.1088/1742-6596/851/1/012005.

[22] H. Watanabe, E. Honda, A. Tetsumura, and T. Kurabayashi, "A comparative study for spatial resolution and subjective image characteristics of a multi-slice ct and a cone-beam CT for dental use," *European Journal of Radiology*, vol. 77, no. 3, pp. 397–402, Mar. 2011, doi: 10.1016/j.ejrad.2009.09.023.

[23] N. Lasiyah, C. Anam, E. Hidayanto, and G. Dougherty, "Automated procedure for slice thickness verification of computed tomography images: variations of slice thickness, position from iso-center, and reconstruction filter," *Journal of Applied Clinical Medical Physics*, vol. 22, no. 7, pp. 313–321, Jul. 2021, doi: 10.1002/acm2.13317.

[24] A. Karius and C. Bert, "QAMaster: a new software framework for phantom-based computed tomography quality assurance," *Journal of Applied Clinical Medical Physics*, vol. 23, no. 4, Apr. 2022, doi: 10.1002/acm2.13588.

[25] M. A. Hobson, E. T. Soisson, S. D. Davis, and W. Parker, "Using the ACR CT accreditation phantom for routine image quality assurance on both CT and CBCT imaging systems in a radiotherapy environment," *Journal of Applied Clinical Medical Physics*, vol. 15, no. 4, pp. 226–239, Jul. 2014, doi: 10.1120/jacmp.v15i4.4835.

BIOGRAPHIES OF AUTHORS

Dr. Choirul Anam completed his Ph.D. at the Department of Physics, Bandung Institute of Technology (ITB). He received a master's degree from the University of Indonesia (UI) and a B.Sc. degree from Diponegoro University (UNDIP). He is currently working as a lecturer and researcher at the UNDIP. His research interests are medical image processing and dosimetry for diagnostic radiology, particularly in CT. He is the developer of two software, i.e. IndoseCT (for calculating and managing radiation dose of CT) and IndoQCT (for measuring CT image quality). He can be contacted at email: anam@fisika.fsm.undip.ac.id.

Dewi A. Insiano is a graduate student in the physics master's program at Diponegoro University. She can be contacted at email: dewiangrainiinsiano@students.undip.ac.id.

Dr. Eng. Eko Hidayanto is a lecturer in radiation physics at Diponegoro University. His expertise is in radiation protection and medical materials. He can be contacted at email: ekohidayanto@fisika.fsm.undip.ac.id.

Ariij Naufal [ID] [SC] is a graduate student in the physics master's program at Diponegoro University. He can be contacted at email: ariij.2019@fisika.fsm.undip.ac.id.

Annisa Tenri Maya [ID] [SC] is a medical physicist at LPFK Surakarta. She can be contacted at email: annisatenri@gmail.com.

Tunggul Drajat Mulatomo [ID] [SC] is a medical physicist at LPFK Surakarta. He can be contacted at email: bedjosll2@gmail.com.

Dr. Mohd Hanafi Ali [ID] [SC] is a lecturer at the Faculty of Medicine, Lincoln University College, 47301, Petaling Jaya, Selangor, Malaysia. He can be contacted at email: han434@gmail.com.